Next-to-leading order QCD predictions for γG associated production in the Large Extra Dimensions model at the CERN Large Hadron Colliders

Xiangdong Gao

Institute of Theoretical Physics
Peking University

August, 25, 2009

In collaboration with Prof. Chong Sheng Li, Jun Gao, and Jian Wang

Outline

Introduction

Introduction

- The large extra dimensions model(LED) is a challenging model at the LHC era, its physical effects can appear at TeV scale, which make searching for extra dimensions models a major task of the LHC.
- γG associated production at the LHC may be a interesting way to directly search for signal of the extra dimensions for it is clean at hadron colliders.
- In order to improve theoretical predictions, NLO QCD calculations are necessary.

Related works

- Tree level investigations.
  G. F. Giudice *et al*, Nucl. Phys. B 544 (1999), 3-38

- Search the signal at Tevatron
  D0, PRL 101, 011601(2008). Their work set limits on M_D, this lower limits on M_D is from 884 to 778GeV for $\delta = 2 \sim 8$.
- Work on QCD corrections in extra dimension models
  P. Mathews, *et al*, Nucl. Phys. B 713(2005)333-377
  P. Mathews, *et al*, JHEP 10(2005)031
  Qiang Li, Chong Sheng Li, Li Lin Yang, Phys. Rev. D74: 056002, 2006. In this work, resummation effects are considered.

The Large Extra Dimension model

The LED model

- The dimension of spacetime is extended to $D = 4 + \delta$
- The SM particles live on the brane, while the graviton propagate in the additional δ-dimensional space, which is assumed for simplicity to be compactified on the δ-dimensional torus with a common radius R.
- The 4-dimensional Planck scale M_P is related to the fundamental scale M_D by

$$M_P^2 = M_D^{\delta+2}(2\pi R).$$

  where $M_D \sim$TeV.
- For $\delta \geq 2$, the LED model is consistent with the current experiments since gravitional force is not well probed at sub-millimeter.

The LED model

- The collider way to search the LED model can be divided into:
  - Missing energy;
  - Virtual effects.
- $\frac{1}{M_P}$ couplings, but infinite KK modes, which leads to observable effects.

Graviton mass splitting

The graviton KK modes have masses equal to $|n|/R$, and their mass splittings are

$$\Delta m \sim \frac{1}{R} = M_D(\frac{M_D}{\bar{M}_P})^{2/\delta} \sim (\frac{M_D}{TeV})^{\frac{2+\delta}{2}} 10^{\frac{12\delta-31}{\delta}} eV$$

So, if $M_D = 1 TeV$ and $\delta = 2, 4, 6$, then Δm equal to 20keV, 7MeV, 0.1GeV. Only large δ have large mass splitting. However, because of the small couplings, if only a small number of KK modes are produced, the total cross section is negligible. In this work, we concentrate on $\delta = 2, 4$.

Graviton mass splitting

We sum up all the KK modes in experimental applications. Because of the small mass splitting, the summation can be replaced by integration. The number of KK modes between $|n|$ and $|n| + d|n|$ is

$$dN = S_{\delta-1}|n|^{\delta-1}dn, \quad S_{\delta-1} = \frac{2\pi^{\delta/2}}{\Gamma\delta/2},$$

where $S_{\delta-1}$ is the surface of a unit-radius sphere in δ dimension, dN can be further connected with mass of KK modes($m = |n|/R$) by:

$$dN = S_{\delta-1}\frac{\bar{M}_P^2}{M_D^{2+\delta}}m^{\delta-1}dm.$$

So, the cross section for inclusive graviton production can be expressed as

$$\sigma = \int S_{\delta-1}\frac{\bar{M}_P^2}{M_D^{2+\delta}}m^{\delta-1}\sigma_m dm \tag{1}$$

where σ_m is the cross section for producing a single graviton of mass m.

Next-to-leading order calculations

Tree-level Feynman diagrams

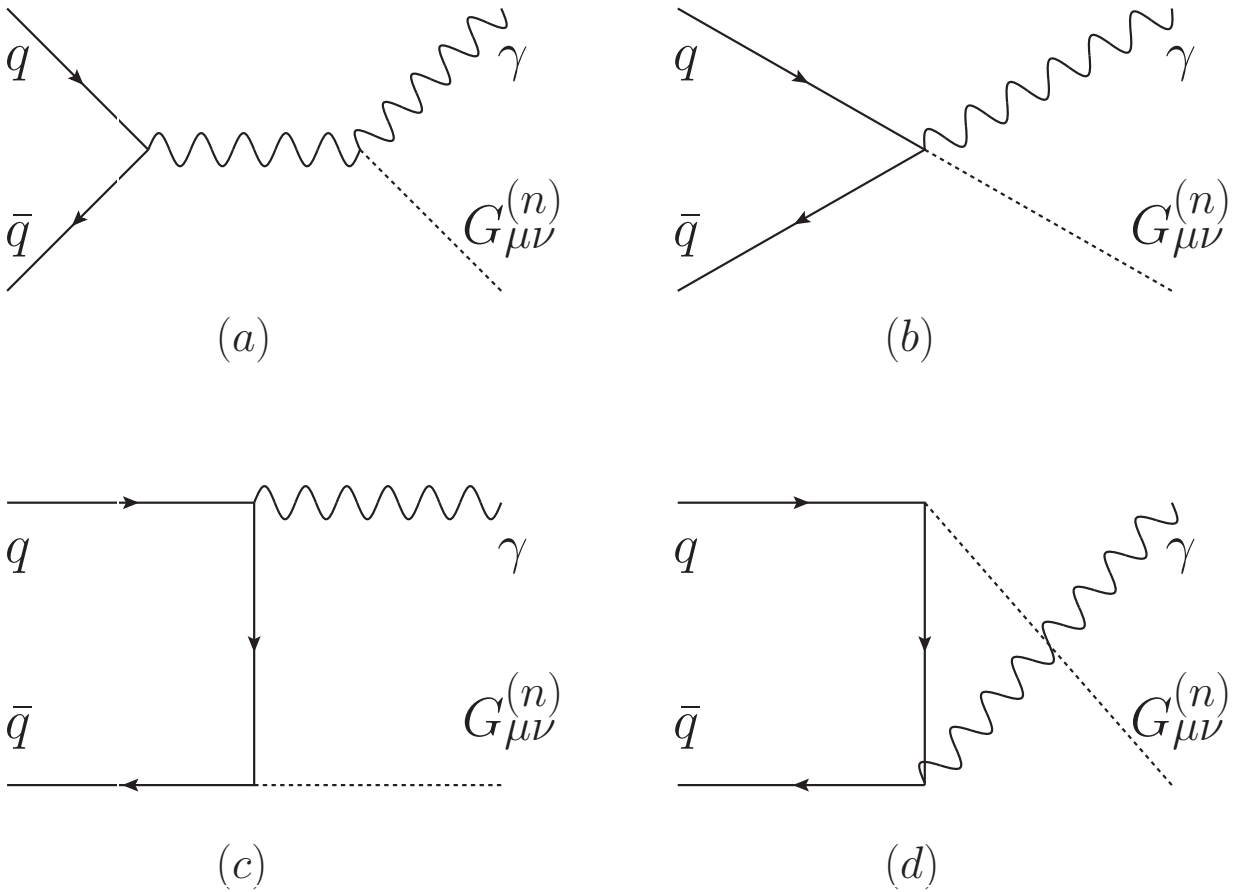

Figure: Leading order Feynman diagrams for $q\bar{q} \to \gamma G$.

NLO calculations

- The NLO contributions for the γG associated production can be separated into virtual corrections arising from the loop diagrams and real contributions arising from the radiation of a real gluon or a massless (anti)quark.
- The dimensional regularization is employed to regulate ultraviolet, soft and collinear divergence in the virtual loop corrections.
- We use two cutoff phase slicing method to handle soft and collinear divergence in real emission processes.

One-loop virtual diagrams

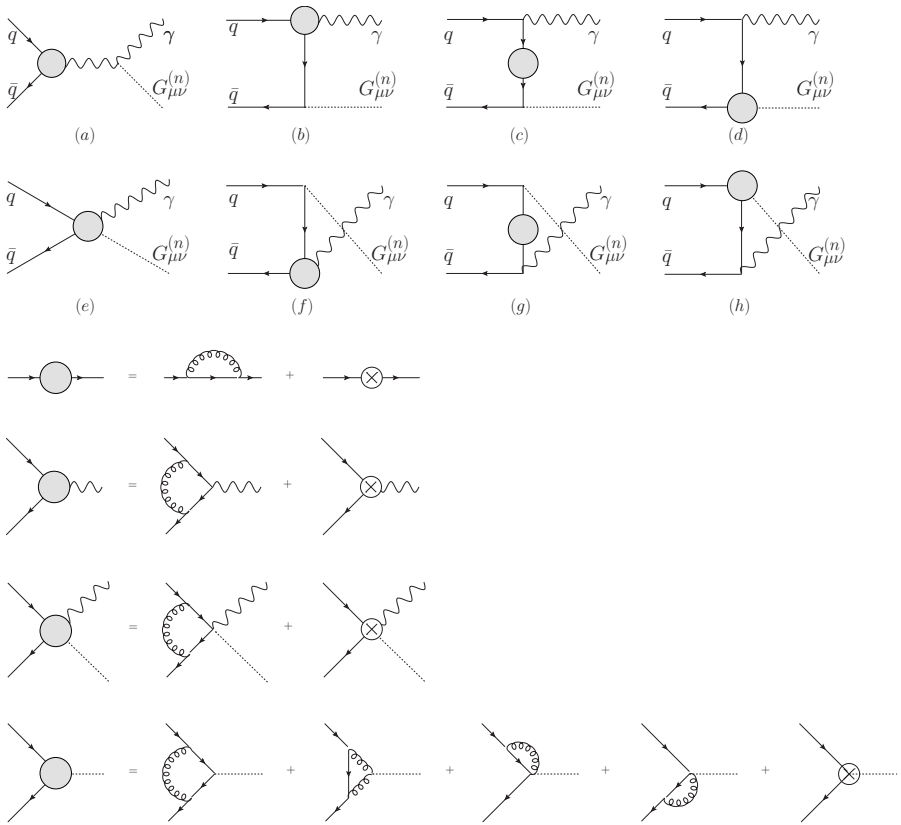

Figure: One-loop virtual diagrams, including vertex and self-energy corrections for $q\bar{q} \longrightarrow \gamma G$. Each brown vertex is UV divergence free.

Box and non-vertex type triangle diagrams

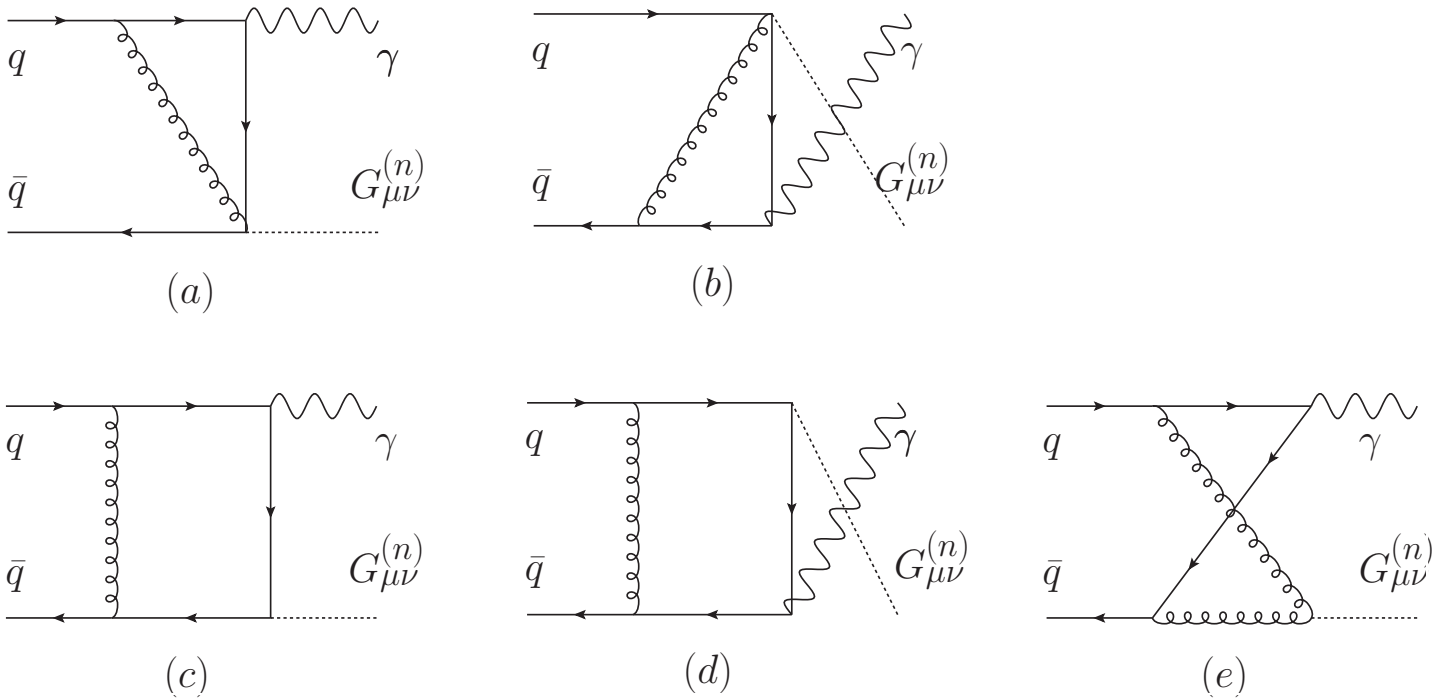

Figure: Box and non-vertex type triangle diagrams for $q\bar{q} \to \gamma G$. The UV divergence cancels each other in the five diagrams.

Virtual corrections

- Because the qqG and ggG vertex have momentum in the Feynman rules, so the box diagrams contribute integration of the following kind:

$$\int \frac{d^n k}{(2\pi)^n} \frac{k^\mu k^\nu k^\rho k^\sigma}{k^2 (k+p1)^2 (k+p2)^2 (k+p3)^2}.$$

  tensor type integration of four index lead to too many terms.
- So, we do not integrate k first, but multiply with tree level amplitude first and then integrate.
- The virtual corrections:

$$2\overline{\sum} M^B M^{V*} = \frac{\alpha_s}{2\pi} \frac{\Gamma(1-\epsilon)}{\Gamma(1-2\epsilon)} \left(\frac{4\pi\mu_r^2}{s}\right)^\epsilon \left(\frac{2A_2^V}{\epsilon^2} + \frac{2A_1^V}{\epsilon} + 2A_0^V\right) \hat{\sigma}^B \quad (2)$$

  where

$$A_2^V = -C_F, \qquad A_1^V = -\frac{3}{2} C_F.$$

Real gluon emission and two cut-offs

- The phase space integration for the real gluon emission will produce infrared singularities, which can be either soft or collinear and can be isolated by slicing the phase space into three different regions defined by two small cut-offs δ_s and δ_c. In each region the divergence can be obtained by analytical integration and the non-divergence term can be obtained by numerical integration.
- The rest collinear divergences can be absorbed into the redefinition of the PDF at NLO, in general called mass factorization.

Real gluon emission and two cut-offs

- An soft cut-off δ_s, according to whether the energy of the emitted gluon is soft, i.e., $E_5 < \delta_s\sqrt{s}/2$ or $E_5 > \delta_s\sqrt{\hat{s}}/2$ separate the phase space and consequently the cross section into two parts:

$$\hat{\sigma}^R = \hat{\sigma}^S + \hat{\sigma}^H, \tag{3}$$

  where $\hat{\sigma}^S$ contains all the soft divergences.

- An collinear cut-off δ_c, according to whether the emitted gluon is collinear to one of the incoming partons, i.e.,$-\delta_c\hat{s} < (p_{1,2} - p_5)^2 < 0$ or not, further separate the hard regions into two parts:

$$\hat{\sigma}^H = \hat{\sigma}^{HC} + \hat{\sigma}^{\overline{HC}}, \tag{4}$$

  where the hard collinear part $\hat{\sigma}^{HC}$ contains the collinear divergence.

Real (anti)quark emission

- In addition to the real gluon emission, there are also massless (anti)quark emission.
- We also use two cut-off phase space slicing method to isolate the initial collinear divergence.
- No soft divergence exists here, so we only sperate the region into two parts: collinear region and non-collinear region.
- $\hat{\sigma}^{\overline{C}}$ can be obtained numerically.

Mass factorization

After adding the renormalized virtual corrections and the real corrections, the partonic cross sections still contain the collinear divergences, which can be absorbed into the redefinition of the PDF at NLO, in general called mass factorization. In the $\overline{\rm MS}$ scheme, the scale dependent PDF $G_{\alpha/p}(x,\mu_f)$ is given by

$$G_{\alpha/p}(x,\mu_f) = G_{\alpha/p}(x) + \sum_\beta (-\frac{1}{\epsilon})\left[\frac{\alpha_s}{2\pi}\frac{\Gamma(1-\epsilon)}{\Gamma(1-2\epsilon)}\left(\frac{4\pi\mu_r^2}{\mu_f^2}\right)^\epsilon\right] \int_x^1 \frac{dz}{z} P_{\alpha\beta}(z) G_{\beta/p}(x/z).$$

Soft part

By factoring $2 \to 3$ matrix element squared into Born matrix element squared times eikonal factor, we can get the analytical result of soft part:

$$\hat{\sigma}^S = \hat{\sigma}^B \left[\frac{\alpha_s}{2\pi} \frac{\Gamma(1-\epsilon)}{\Gamma(1-2\epsilon)} \left(\frac{4\pi\mu_r^2}{s} \right)^{\epsilon} \right] \left(\frac{A_2^s}{\epsilon^2} + \frac{A_1^s}{\epsilon} + A_0^s \right) \tag{5}$$

with

$$A_2^s = 2C_F, \quad A_1^s = -4C_F \log \delta_s, \quad A_0^s = 4C_F \log^2 \delta_s. \tag{6}$$

Collinear part

The collinear part can be obtained by factoring $2 \to 3$ matrix element squared into Born matrix element squared times Altarelli-Parisi splitting function. After the redefinition of the parton PDF, we have

$$\sigma^{coll} = \int \hat{\sigma}^B \left[\frac{\alpha_s}{2\pi} \frac{\Gamma(1-\epsilon)}{\Gamma(1-2\epsilon)} \left(\frac{4\pi\mu_r^2}{s} \right)^{\epsilon} \right] \{ \tilde{G}_{q/p}(x_1, \mu_f) G_{\bar{q}/p}(x_2, \mu_f) +$$
$$G_{q/p}(x_1, \mu_f) \tilde{G}_{\bar{q}/p}(x_2, \mu_f) + \sum_{\alpha=q,\bar{q}} \left[\frac{A_1^{sc}(\alpha \to \alpha g)}{\epsilon} + A_0^{sc}(\alpha \to \alpha g) \right]$$
$$G_{q/p}(x_1, \mu_f) G_{\bar{q}/p}(x_2, \mu_f) + (x_1 \leftrightarrow x_2) \} dx_1 dx_2, \tag{7}$$

where

$$A_1^{sc}(q \to qg) = A_1^{sc}(\bar{q} \to \bar{q}g) = C_F(2 \ln \delta_s + 3/2), \tag{8}$$
$$A_0^{sc} = A_1^{sc} \ln(\frac{s}{\mu_f^2}), \tag{9}$$
$$\tilde{G}_{\alpha(=q,\bar{q})/p}(x, \mu_f) = \sum_{\beta=g,\alpha} \int_x^{1-\delta_s\delta_{\alpha\beta}} \frac{dy}{y} G_{\beta/p}(x/y, \mu_f) \tilde{P}_{\alpha\beta}(y) \tag{10}$$

Collinear part

$$\tilde{P}_{\alpha\beta}(y) = P_{\alpha\beta}(y)\ln(\delta_c \frac{1-y}{y}\frac{s}{\mu_f^2}) - P'_{\alpha\beta}(y),$$

with

$$P_{qq}(z) = P_{\bar{q}\bar{q}}(z) = C_F\frac{1+z^2}{1-z} + C_F\frac{3}{2}\delta(1-z),$$
$$P'_{qq}(z) = P'_{\bar{q}\bar{q}}(z) = -C_F(1-z) + C_F\frac{1}{2}\delta(1-z);$$

and

$$\begin{aligned} P_{qg}(z) &= P_{\bar{q}g}(z) = \frac{1}{2}[z^2+(1-z)^2], \\ P'_{qg}(z) &= P'_{\bar{q}g}(z) = -z(1-z). \end{aligned}$$

Total NLO cross section

The NLO total cross section for $pp \to \gamma G$ in the $\overline{MS}$ factorization scheme is obtained by summing up the Born, virtual, soft, collinear and hard non-collinear contributions.

$$\begin{aligned}\sigma^{NLO} = & \int dx_1 dx_2 \{ \Big[G_{q/p}(x_1,\mu_f) G_{\bar{q}/p}(x_2,\mu_f) + (x_1 \leftrightarrow x_2) \Big] (\hat{\sigma}^B + \hat{\sigma}^V + \hat{\sigma}^S + \hat{\sigma}^{\overline{HC}}) \} \\ & + \sum_{(\alpha=g,\beta=q,\bar{q})} \int dx_1 dx_2 \Big[G_{\alpha/p}(x_1,\mu_f) G_{\beta/p}(x_2,\mu_f) + (x_1 \leftrightarrow x_2) \Big] \hat{\sigma}^{\overline{C}}(\alpha\beta \to G\gamma + X) \\ & + \sigma^{coll} . \end{aligned} \tag{11}$$

Cancelation of soft and collinear divergence

All the divergence cancel in σ^{NLO}

$$\frac{1}{\epsilon^2} \quad : \quad 2A_2^V + A_2^s = 0$$

$$\frac{1}{\epsilon} \quad : \quad 2A_1^V + A_1^s + A_1^{sc}(q \to qg) + A_1^{sc}(\bar{q} \to \bar{q}g) = 0$$

Numerical results

δ_s dependence

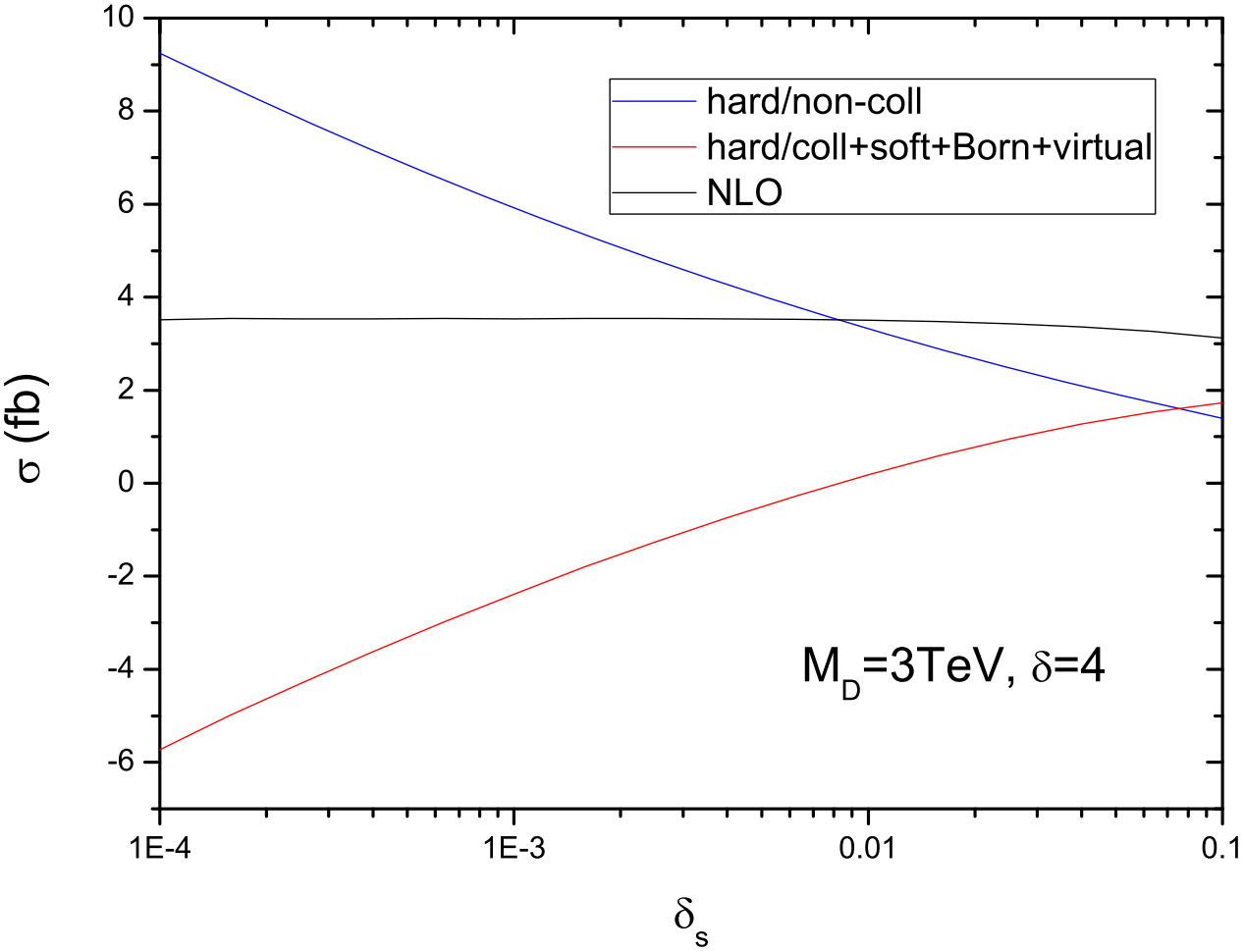

Figure: Dependence of the NLO total cross sections for the γG associated production at the LHC on the theoretical cutoff δ_s with $\delta_c = \delta_s/50$, assuming $M_D = 3\text{TeV}$, $\delta = 4$.

Scale dependence

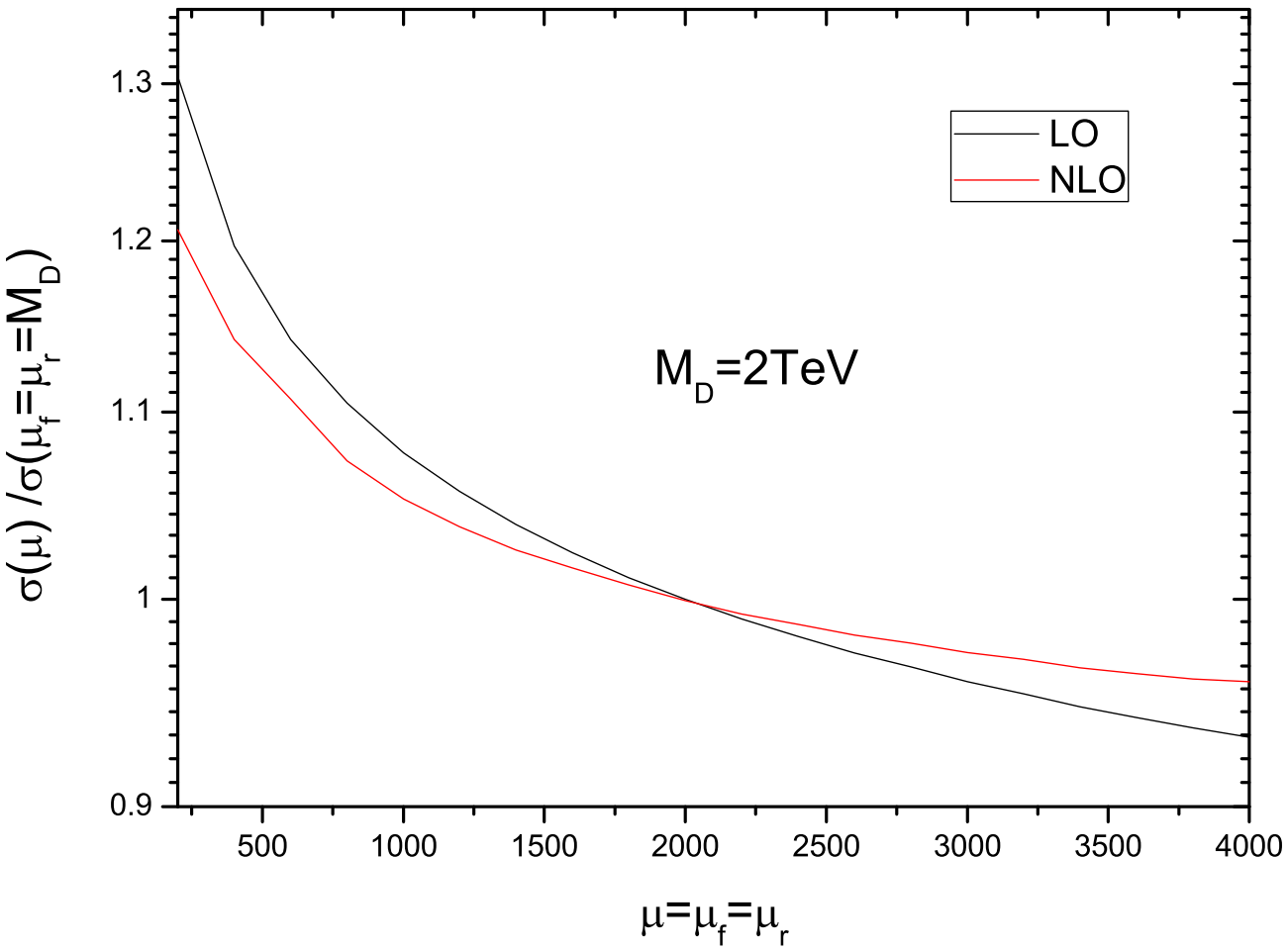

Figure: Dependence of the NLO total cross sections for the γG associated production at the LHC on the factorization scale(μ_f) and the renormalization scale(μ_r), assuming $M_D = 3\text{TeV}$, $\delta = 4$.

Total cross section versus M_D

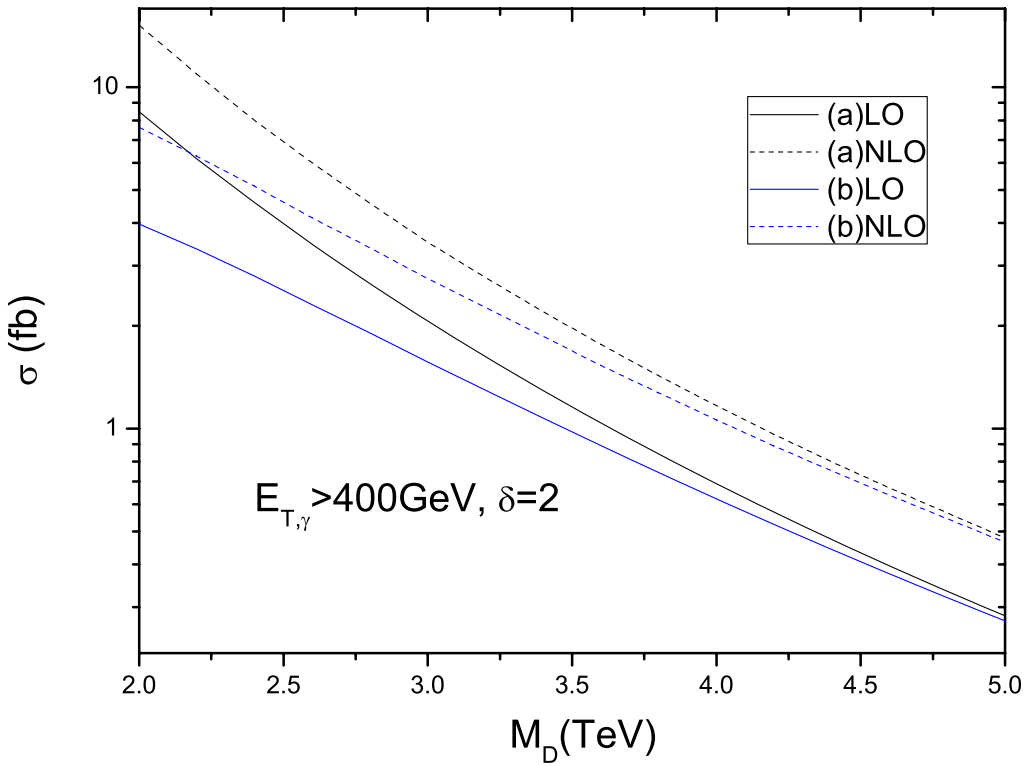

Figure: Dependence of the total cross section of the γG associated production at the LHC on M_D , assuming $\delta = 2$, and also with the requirement that $E_{T,\gamma} > 400\text{GeV}$, $|\eta| < 2.5$, $p_{T,G} > 100\text{GeV}$, and $\Delta R > 0.4$. The a and b lines are constructed by integrating the cross section over all $m_{\gamma G}$ and $m^2_{\gamma G} < M^2_D$, respectively, where $m_{\gamma G}$ is the invariant mass of γ and graviton.

K factor versus M_D

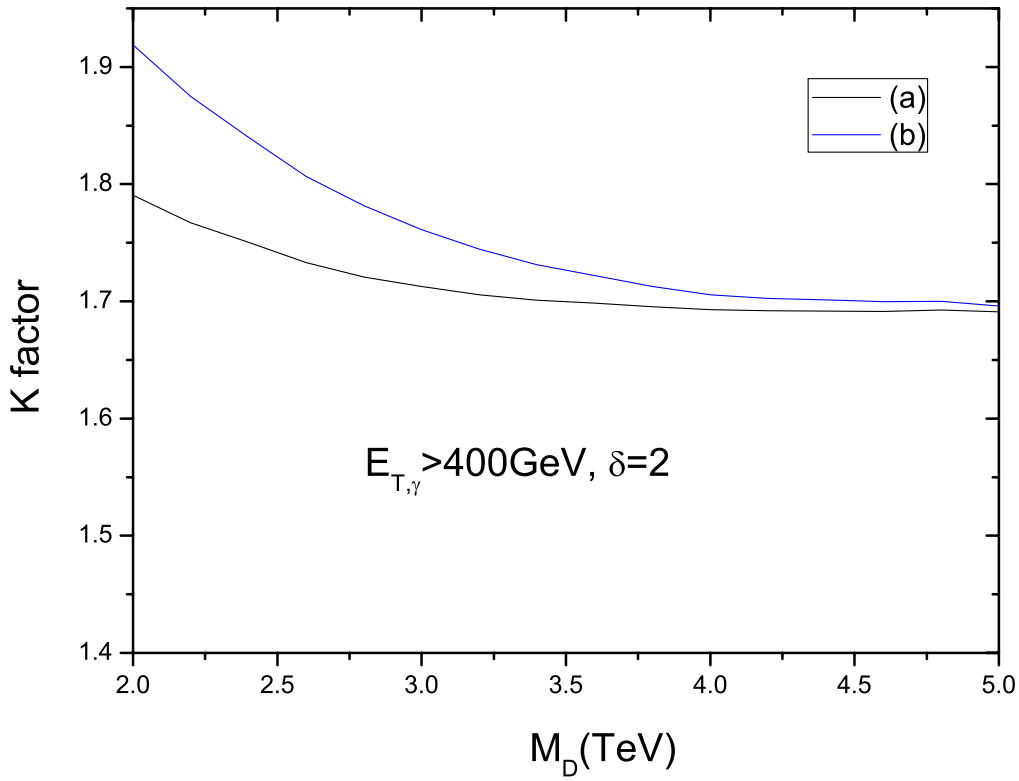

Figure: K factor, defined as σ_{NLO}/σ_{LO}, for the γG associated production at the LHC on M_D , assuming $\delta = 2$, and also with the requirement that $E_{T,\gamma} > 400\text{GeV}$, $|\eta| < 2.5$, $p_{T,G} > 100\text{GeV}$, and $\Delta R > 0.4$. The *a* and *b* lines are constructed by integrating the cross section over all $m_{\gamma G}$ and $m^2_{\gamma G} < M^2_D$, respectively, where $m_{\gamma G}$ is the invariant mass of γ and graviton.

Total cross section versus M_D

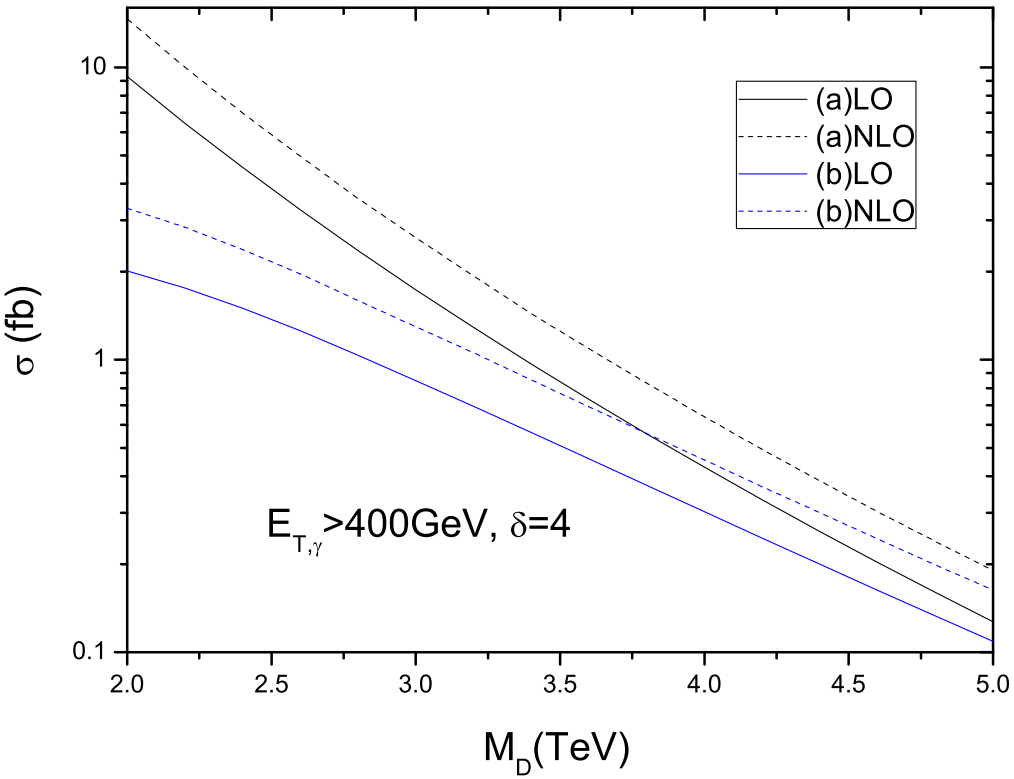

Figure: Dependence of the total cross section of the γG associated production at the LHC on M_D , assuming $\delta = 4$, and also with the requirement that $E_{T,\gamma} > 400\text{GeV}$, $|\eta| < 2.5$, $p_{T,G} > 100\text{GeV}$, and $\Delta R > 0.4$. The a and b lines are constructed by integrating the cross section over all $m_{\gamma G}$ and $m^2_{\gamma G} < M^2_D$, respectively, where $m_{\gamma G}$ is the invariant mass of γ and graviton.

K factor versus M_D

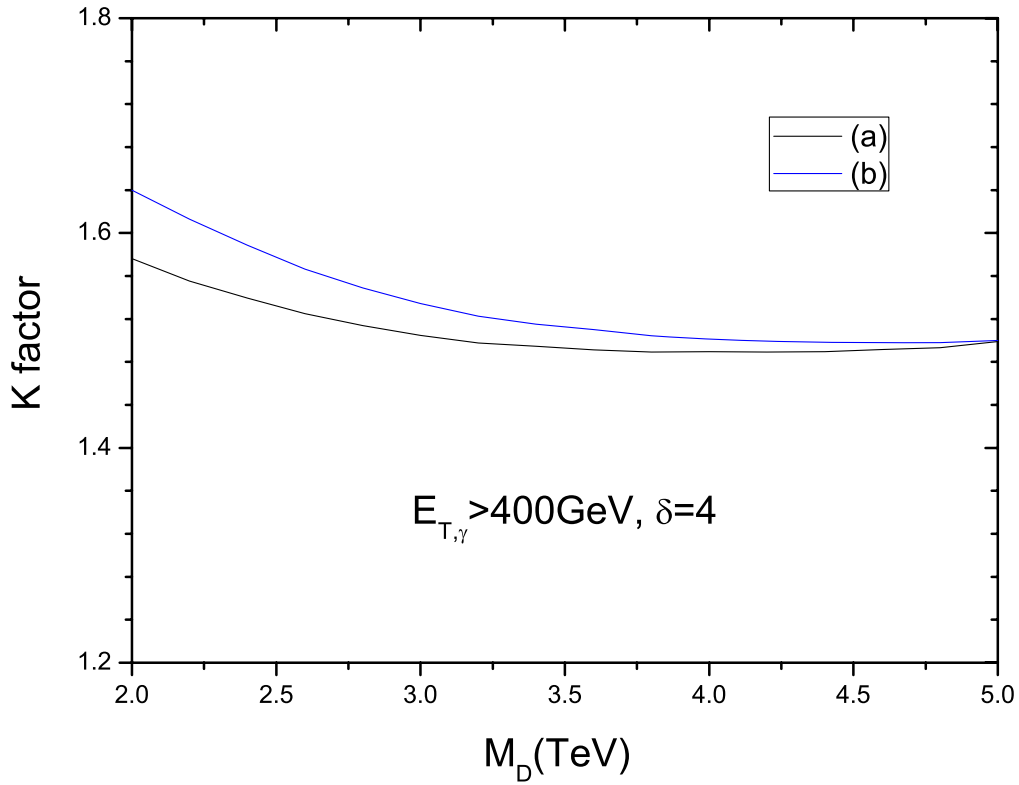

Figure: K factor, defined as σ_{NLO}/σ_{LO}, for the γG associated production at the LHC on M_D , assuming $\delta = 4$, and also with the requirement that $E_{T,\gamma} > 400\text{GeV}$, $|\eta| < 2.5$, $p_{T,G} > 100\text{GeV}$, and $\Delta R > 0.4$. The *a* and *b* lines are constructed by integrating the cross section over all $m_{\gamma G}$ and $m^2_{\gamma G} < M^2_D$, respectively, where $m_{\gamma G}$ is the invariant mass of γ and graviton.

Total cross section versus $E_{T,\gamma}^{min}$

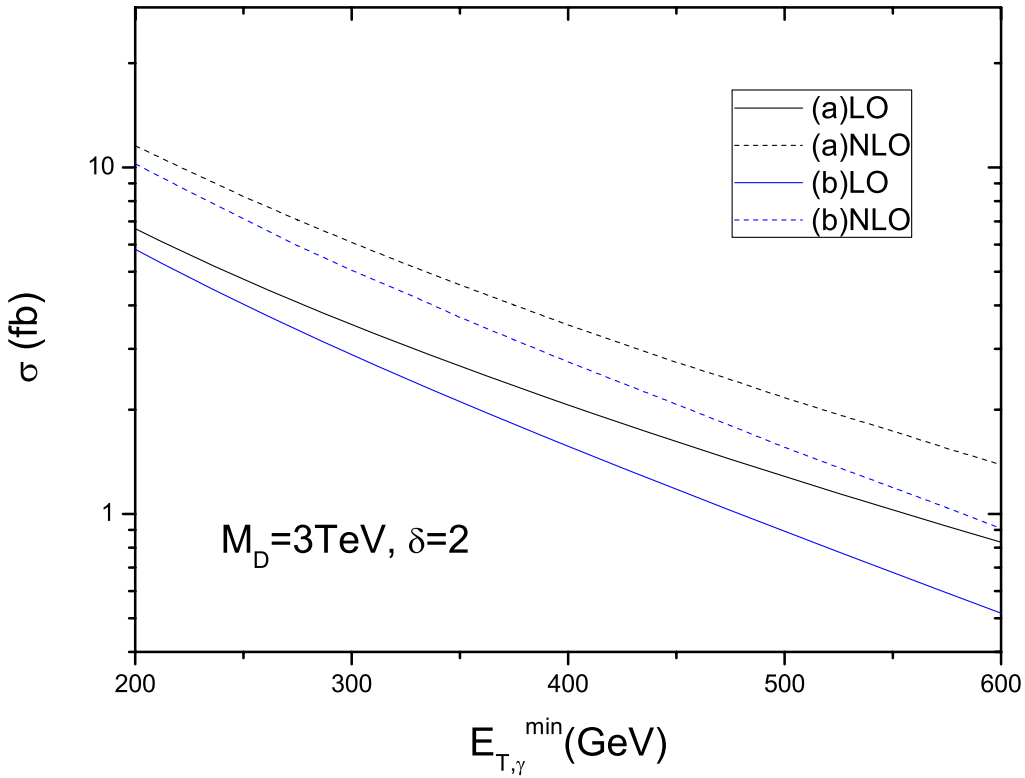

Figure: Dependence of the total cross section of the γG associated production at the LHC on $E_{T,\gamma}^{min}$, assuming $M_D = 3\text{TeV}$, $\delta = 2$, and also with the requirement that $|\eta| < 2.5$, $p_{T,G} > 100\text{GeV}$, and $\Delta R > 0.4$. The *a* and *b* lines are constructed by integrating the cross section over all $m_{\gamma G}$ and $m_{\gamma G}^2 < M_D^2$, respectively, where $m_{\gamma G}$ is the invariant mass of γ and graviton.

K factor versus $E_{T,\gamma}^{min}$

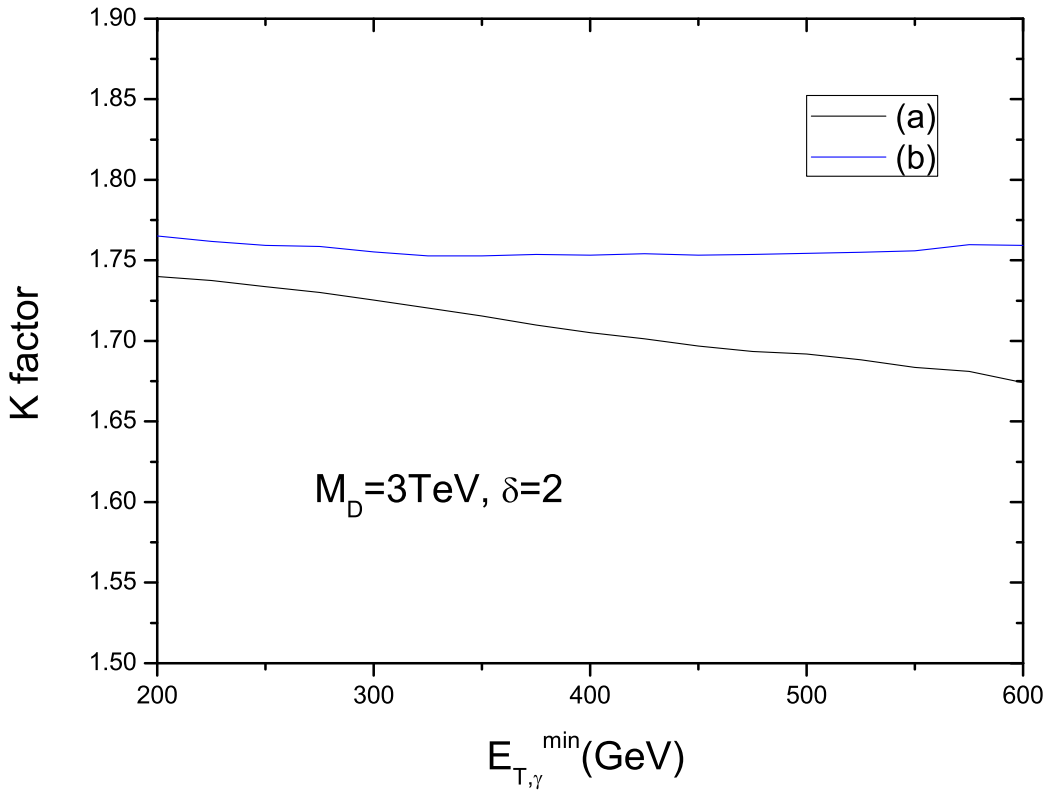

Figure: K factor, defined as σ_{NLO}/σ_{LO}, for the γG associated production at the LHC on $E_{T,\gamma}^{min}$, assuming $M_D = 3\text{TeV}$, $\delta = 2$, and also with the requirement that $|\eta| < 2.5$, $p_{T,G} > 100\text{GeV}$, and $\Delta R > 0.4$. The a and b lines are constructed by integrating the cross section over all $m_{\gamma G}$ and $m_{\gamma G}^2 < M_D^2$, respectively, where $m_{\gamma G}$ is the invariant mass of γ and graviton.

Total cross section versus $E_{T,\gamma}^{min}$

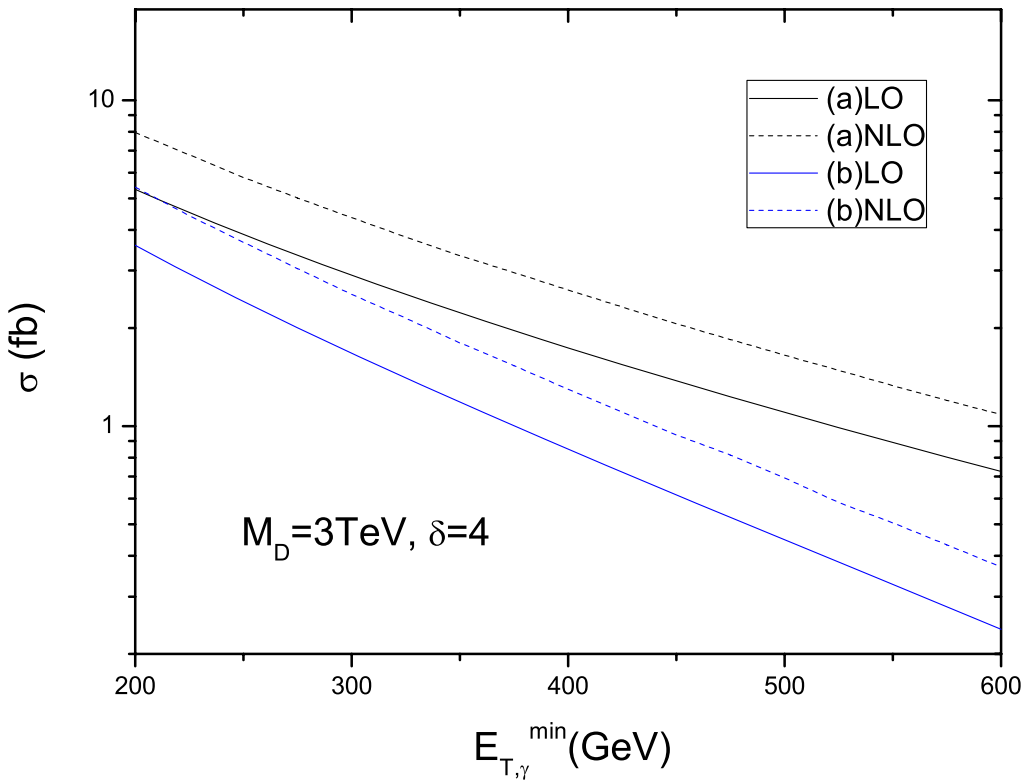

Figure: Dependence of the total cross section of the γG associated production at the LHC on $E_{T,\gamma}^{min}$, assuming $M_D = 3\text{TeV}$, $\delta = 4$, and also with the requirement that $|\eta| < 2.5$, $p_{T,G} > 100\text{GeV}$, and $\Delta R > 0.4$. The *a* and *b* lines are constructed by integrating the cross section over all $m_{\gamma G}$ and $m_{\gamma G}^2 < M_D^2$, respectively, where $m_{\gamma G}$ is the invariant mass of γ and graviton.

K factor versus $E_{T,\gamma}^{min}$

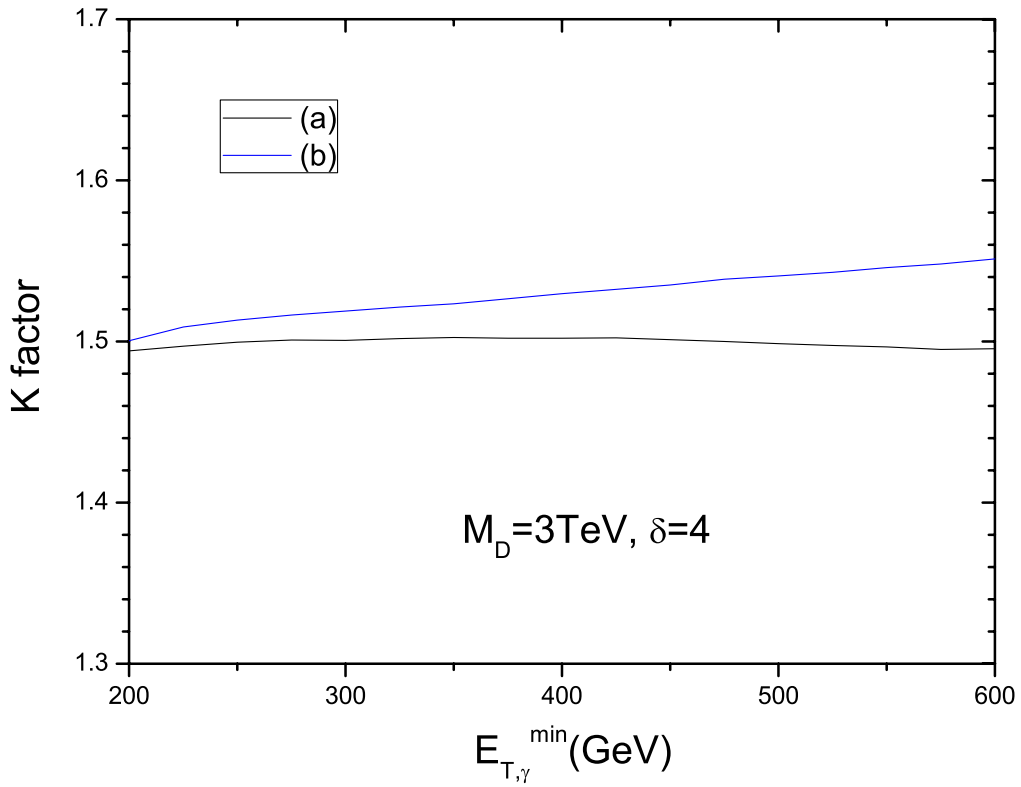

Figure: K factor, defined as σ_{NLO}/σ_{LO}, for the γG associated production at the LHC on $E_{T,\gamma}^{min}$, assuming $M_D = 3\text{TeV}$, $\delta = 4$, and also with the requirement that $|\eta| < 2.5$, $p_{T,G} > 100\text{GeV}$, and $\Delta R > 0.4$. The a and b lines are constructed by integrating the cross section over all $m_{\gamma G}$ and $m_{\gamma G}^2 < M_D^2$, respectively, where $m_{\gamma G}$ is the invariant mass of γ and graviton.

Differential cross section versus $E_{T,\gamma}$

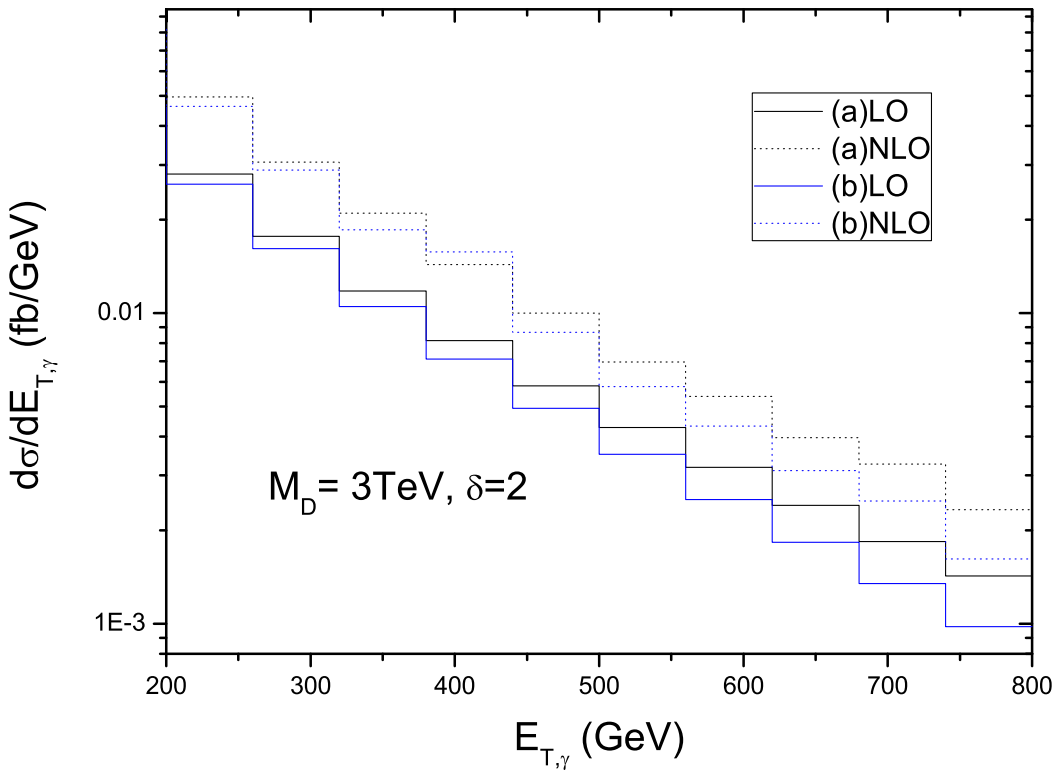

Figure: Dependence of the differential cross section of the γG associated production at the LHC on $E_{T,\gamma}$, assuming $M_D = 3\text{TeV}$ and $\delta = 2$, and also with the requirement that $|\eta| < 2.5$, $p_{T,G} > 100\text{GeV}$, and $\Delta R > 0.4$. The a and b lines are constructed by integrating the cross section over all $m_{\gamma G}$ and $m^2_{\gamma G} < M^2_D$, respectively, where $m_{\gamma G}$ is the invariant mass of γ and graviton.

Differential cross section versus $E_{T,\gamma}$

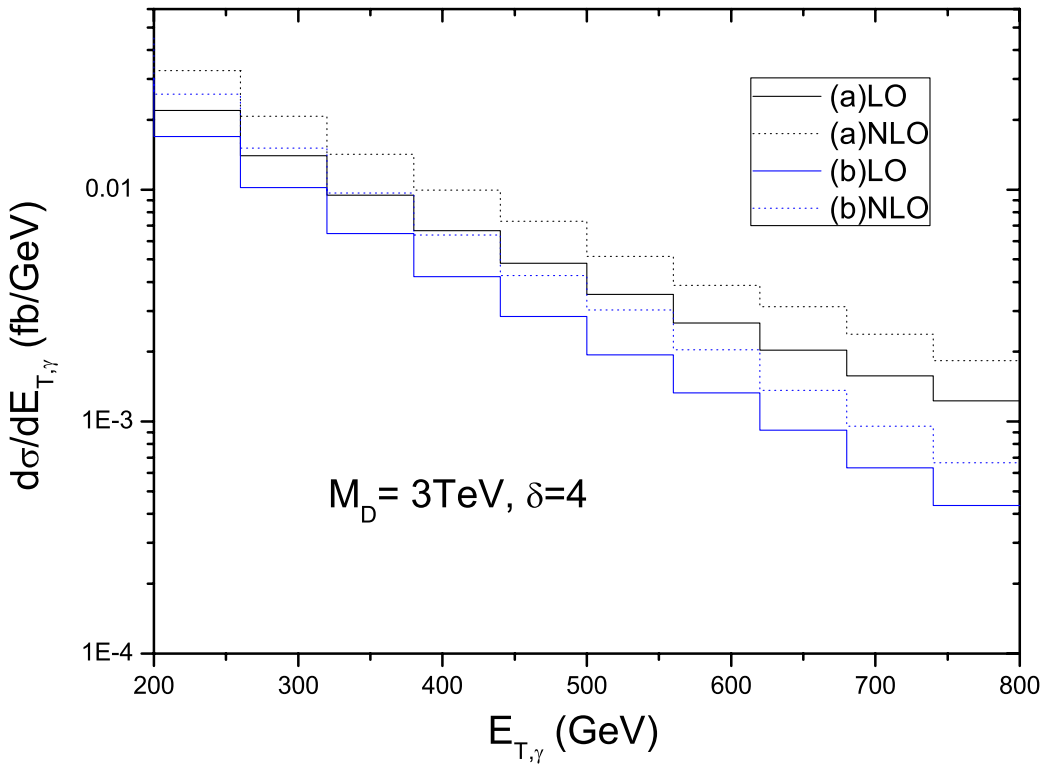

Figure: Dependence of the differential cross section of the γG associated production at the LHC on $E_{T,\gamma}$, assuming $M_D = 3\text{TeV}$ and $\delta = 4$, and also with the requirement that $|\eta| < 2.5$, $p_{T,G} > 100\text{GeV}$, and $\Delta R > 0.4$. The a and b lines are constructed by integrating the cross section over all $m_{\gamma G}$ and $m^2_{\gamma G} < M^2_D$, respectively, where $m_{\gamma G}$ is the invariant mass of γ and graviton.

Differential cross section versus $|\eta|$

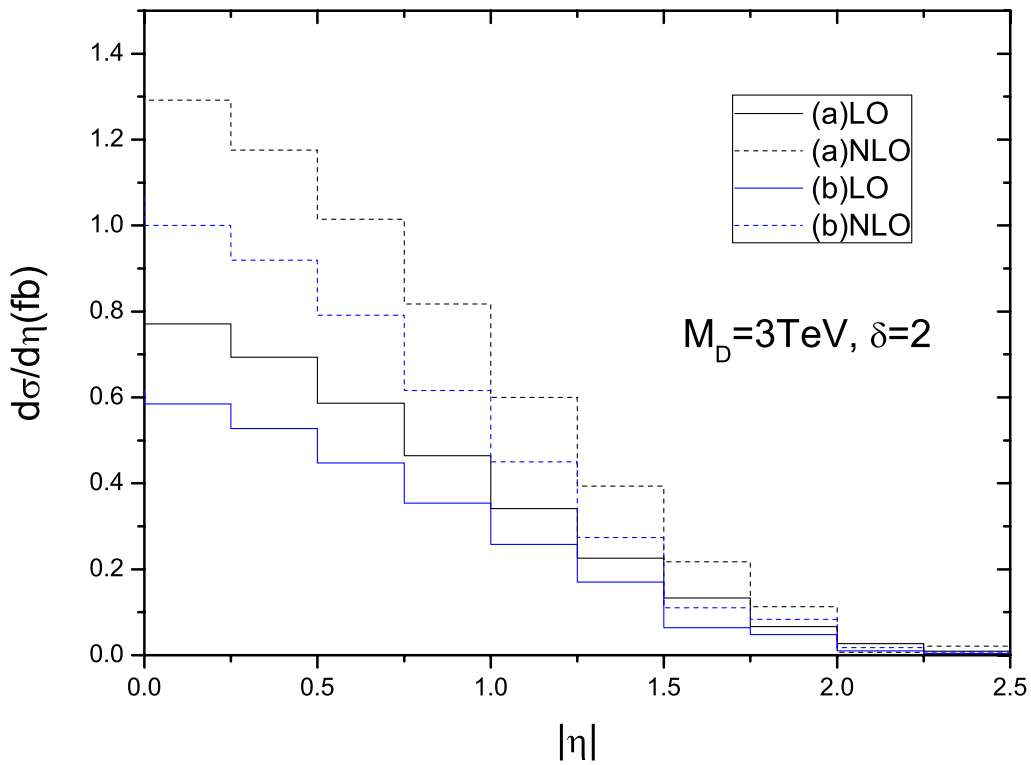

Figure: Dependence of the differential cross section of the γG associated production at the LHC on $|\eta|$, assuming $M_D = 3\text{TeV}$ and $\delta = 2$, and also with the requirement that $E_{T,\gamma} > 400\text{GeV}$, $p_{T,G} > 100\text{GeV}$, and $\Delta R > 0.4$. The *a* and *b* lines are constructed by integrating the cross section over all $m_{\gamma G}$ and $m^2_{\gamma G} < M^2_D$ respectively, where $m_{\gamma G}$ is the invariant mass of γ and graviton.

Differential cross section versus $|\eta|$

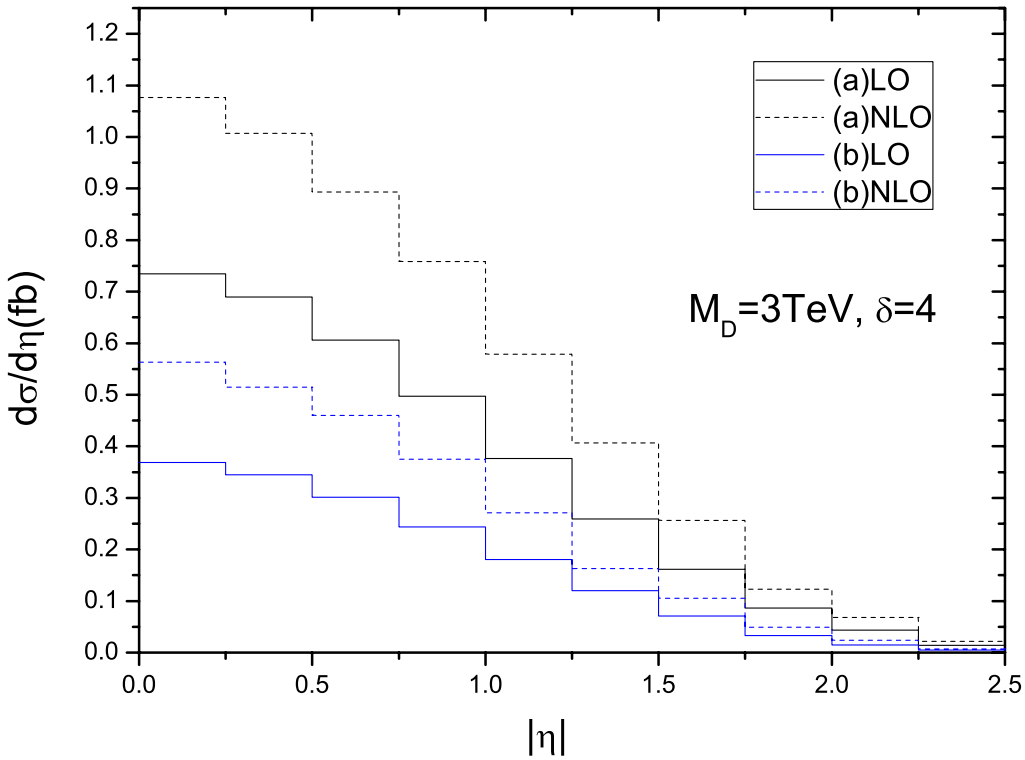

Figure: Dependence of the differential cross section of the γG associated production at the LHC on $|\eta|$, assuming $M_D = 3\text{TeV}$ and $\delta = 4$, and also with the requirement that $E_{T,\gamma} > 400\text{GeV}$, $p_{T,G} > 100\text{GeV}$, and $\Delta R > 0.4$. The a and b lines are constructed by integrating the cross section over all $m_{\gamma G}$ and $m^2_{\gamma G} < M^2_D$ respectively, where $m_{\gamma G}$ is the invariant mass of γ and graviton.

Summary

Summary

- We calculated the next-to-leading order QCD corrections for the γG associated production at the LHC in the LED model.
- The NLO corrections efficiently reduce the dependence of the total cross sections on the renormalization/factorization scale.
- Our numerical results show that the total cross sections can be significantly enhanced by the NLO corrections, the K factor is around $1.6 \sim 1.8$ when $\delta = 2$. For larger δ, e.g.,4, K factor reduced to $1.5 \sim 1.6$.
- We also examined differential distributions and found that the NLO QCD corrections is almost the same in different regions.

Thank You !